

Study on the Frequency Dependence of Harmonic Current

Jong Jip Kim*, Yu Mi Young

Korea Research Institute of Standards and Science, Doryong dong 1, Yusong, TaeJön, 305-600, Korea

*E-mail: jjkim@kriss.re.kr

Received: 17 July 2014 / Accepted: 8 September 2014 / Published: 29 September 2014

Harmonic current was measured for a type 316 stainless steel to investigate the effects of frequency on the harmonic current in NaCl solutions with pH 1.6 and 1.9. Harmonic current increases, and polarization resistance decreases with increasing frequency in both solutions in charge transfer condition. The increase in harmonic current with frequency was also observed in mixed control condition of charge transfer and diffusion. The square of harmonic current is linearly dependent on that of frequency in charge transfer condition, but not in mixed control condition. To fit the experimental data in the latter condition, a simple relation was developed by a dimensional analysis. According to the equation developed, the square of harmonic current is linearly dependent upon the frequency in mixed control condition.

Keywords: harmonic current, 316 stainless steel, corrosion, charge transfer, diffusion

1. INTRODUCTION

Distortion of current appears with respect to the voltage when the electrode is polarized with sinusoidal voltage. The distortion is caused by the non-linearity of the current-potential characteristics of electrode-solution interface. The current generally consists of a component of the same frequency as well as terms at integral multiples of the input frequency, but with shift in phase with respect to the voltage, the harmonics. The current also comprises a DC offset, the zeroth harmonic. The knowledge of the amplitude of harmonic currents allows obtaining the corrosion rate and Tafel parameters within one measurement [1].

Determination of corrosion rate by harmonic analysis or harmonic current measurement has been reported in various corrosion systems such as mild steel [2-5], iron [6,7], zinc [8], copper [8,9], rebar in concrete [10-12] as well as iron in media containing inhibitors [13]. Though the harmonic current and corrosion current density were predicted to be independent of the frequency of potential applied in early works [1,2], they have been reported to be dependent upon the frequency and

amplitude of the applied potential as well. They were reported to increase with increasing either frequency or amplitude of applied potential [11].

The frequency and amplitude of applied potential have been reported in some corrosion systems that give corrosion rate consistent with that from weight loss, linear polarization and electrochemical impedance measurements [4,11]. Corrosion rates determined from harmonic current data at 10 - 100 mHz and 5 - 10 mV were in good agreement with those from other tests [4,7,13].

The frequency dependence of harmonic current has been expressed in mathematical forms. For the case where corrosion reactions are controlled by charge transfer, the square of harmonic current is linearly dependent upon the square of frequency [13], whereas in the case where both the charge transfer and diffusion contribute to the total corrosion reaction, the square of harmonic current is inversely proportional to the square root of frequency [3]. However, the expression in the latter is complicated and includes a special function. Surface concentration profile and diffusion coefficient data of oxidant [3] are needed for the evaluation, and validity evaluation is also necessary in various corrosion systems.

The present investigation was undertaken to study the frequency dependence of harmonic current in a type 316 stainless steel with a focus given to the case where corrosion process is under mixed control of charge transfer and diffusion. Development of a simple relation by dimensional analysis was sought that best fits experimental data.

2. EXPERIMENTAL PROCEDURE

2.1. Specimen preparation

A type 316 stainless steel plate was used with the chemical composition by weight: 0.08 C, 0.44 Si, 0.42 Mn, 0.025 P, 0.001 S, 16.72 Cr, 13.23 Ni, 0.03 Mo and Fe balance. The plate was annealed for 3600 s at 1080 °C and quenched in water. Specimens of disc-type 18 mm in diameter were cut from the plate and mechanically ground to have a thickness of 1.5 mm. The ground surfaces of specimens were polished finally using 1 μ m diamond paste. They were then mounted in a flat specimen holder sealed with a crevice free gasket.

2.2. Electrochemical measurement

Polarization, electrochemical impedance spectroscopy (EIS) and harmonic current measurements were carried out at 23 ± 2 °C in 2 % NaCl solutions with pH 1.6 and 1.9. A conventional three electrode cell was used in a 1 L flask with specimen electrode, platinum counter electrode and saturated calomel electrode. The measurement system employed was G 300 (Gamry Instruments) driven by associated softwares.

In all tests the solution was deaerated before specimen immersion with a pure nitrogen gas, which continued throughout the test. Corrosion potential was measured for 1 hr prior to potentiodynamic, potentiostatic, electrochemical impedance and harmonic current measurements. The

potentiodynamic polarization curves were obtained at a scan rate of 0.6 V/h. EIS data were acquired in the frequency range from 100 kHz to 10 mHz with an amplitude of 10 mV peak to peak for the a.c. signal.

Harmonic current measurements were carried out at the corrosion potential. The measurements were also performed immediately after potentiostatic polarizations at a potential 150 mV more positive than the corrosion potential in which corrosion is shown to occur under mixed control of charge transfer and diffusion. Sinusoidal voltage signals of 10 mV amplitude at frequencies ranging from 10^{-3} to 10^{-1} Hz were applied for all measurements.

2.3. Data analysis

The current response to a voltage perturbation in the vicinity of corrosion potential can be expressed by

$$j = j_{cor}[\exp(\Delta E/\beta_a) - \exp(-\Delta E/\beta_c)] \quad (1)$$

where j is the current density, j_{cor} the corrosion current density, ΔE the overpotential, β_a the anodic and β_c the cathodic Tafel slopes divided by $\ln 10$.

When the electrode is polarized by an alternating potential having amplitude E_o and angular frequency ω , the applied potential or overpotential is given by

$$\Delta E = E_o \sin \omega t \quad (2)$$

Expanding the exponential terms in equation (1) by Fourier series and approximating with Taylor polynomials gives following expressions [1],

$$j_1 = j_{cor} E_o (1/\beta_a + 1/\beta_c) \quad (3)$$

$$j_2 = j_{cor} E_o^2 \{1/\beta_a^2 - 1/\beta_c^2\} / 4 \quad (4)$$

$$j_3 = j_{cor} E_o^3 (1/\beta_a^3 + 1/\beta_c^3) / 24 \quad (5)$$

$$j_{cor} = j_1^2 / (48)^{0.5} (2j_1 j_3 - j_2^2)^{0.5} \quad (6)$$

$$1/\beta_a = 2(j_1/j_{cor} + 4j_2/j_1) / E_o \quad (\text{if } \beta_a < \beta_c) \quad (7a)$$

$$1/\beta_c = 2(j_1/j_{cor} - 4j_2/j_1) / E_o \quad (\text{“ ”}) \quad (7b)$$

or

$$1/\beta_a = 2(j_1/j_{cor} - 4j_2/j_1) / E_o \quad (\text{if } \beta_a < \beta_c) \quad (8a)$$

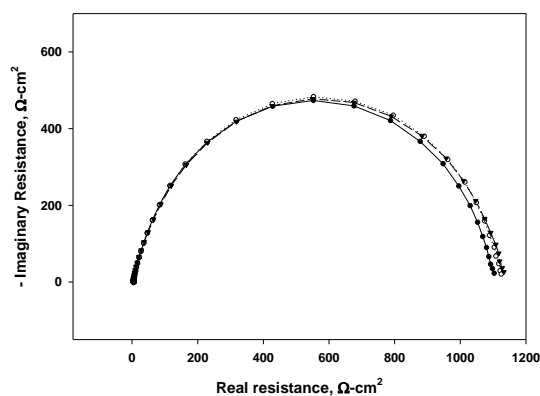
$$1/\beta_c = 2(j_1/j_{cor} + 4j_2/j_1) / E_o \quad (\text{“ ”}) \quad (8b)$$

where j_1 the first harmonic, j_2 the second harmonic, j_3 the third harmonic current density.

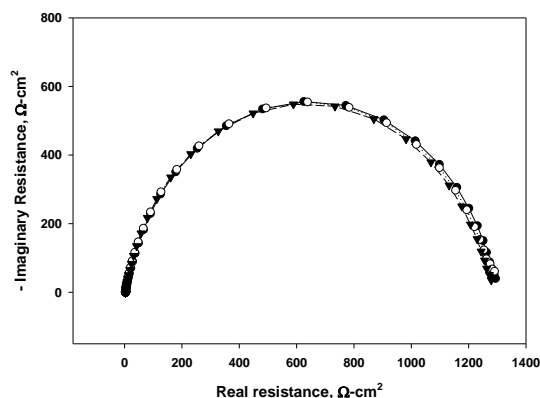
3. RESULTS AND DISCUSSION

3.1. Harmonic current in charge transfer condition

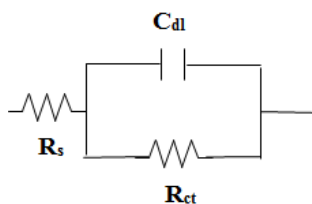
Fig. 1 shows the EIS Nyquist plots obtained after immersion for 3600 s at the corrosion potential in 2.0 % NaCl solutions with pH 1.6 and 1.9. The Nyquist plots are composed of capacitive arcs in this condition, indicating the corrosion process is under charge transfer control. The arc represents the combined effects of electric double layer capacitance C_{dl} and charge transfer resistance R_{ct} , and its diameter is related to the magnitude of charge transfer resistance at the specimen-solution interface. Values of resistance and capacitance were determined by fitting to an equivalent circuit in Fig. 1(c) consisting of solution resistance R_s in series with the parallel combination of the C_{dl} and R_{ct} .



(a)



(b)



(c)

Figure 1. Nyquist plots for a type 316 stainless steel at the corrosion potential in 2 % NaCl solutions with pH 1.6 (a) and 1.9 (b), and an equivalent circuit (c).

The value of R_{ct} is a little higher in the solution with pH 1.9 than that in the solution of pH 1.6 indicating corrosion rate under open circuit condition would be lower in the solution with higher pH. Lowering of polarization resistance in the solution with lower pH is also observed in the d. c. polarization results in Fig. 2.

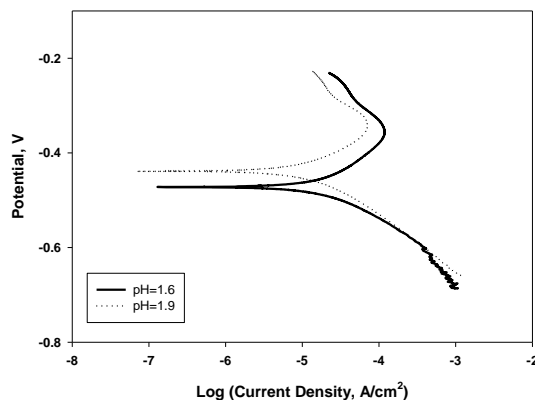
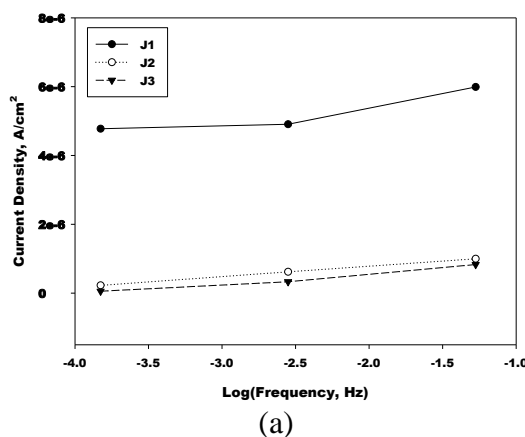


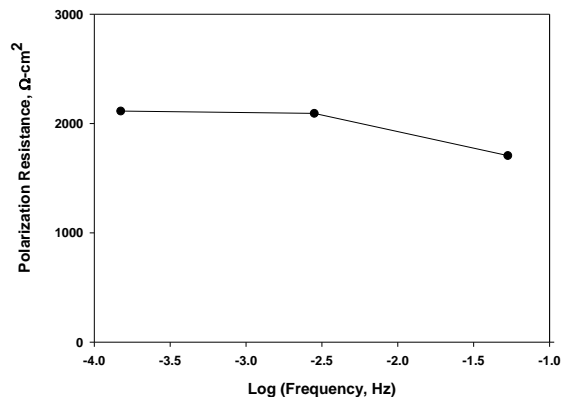
Figure 2. Potentiodynamic polarization plots for a type 316 stainless steel in 2 % NaCl solutions.

Value of polarization resistance is 841.3 and 1108.0 $\Omega\text{-cm}^2$ in 2 % NaCl solutions with pH 1.6 and 1.9, respectively. These are lower compared to those from EIS results, 1149.3 and 1299.7 $\Omega\text{-cm}^2$ in 2 % NaCl solutions with pH 1.6 and 1.9, respectively, indicating that polarization resistance is dependent upon the measurement procedure, that is, a procedural property.

Figs. 3 and 4 represent the results of harmonic current and polarization resistance measurements as a function of frequency at the corrosion potentials in 2 % NaCl solution with pH 1.6 and 1.9, respectively. The corrosion current density and polarization resistance were determined from harmonic current measurements at a sinusoidal potential of 10 mV. Polarization resistance was calculated using a relation,

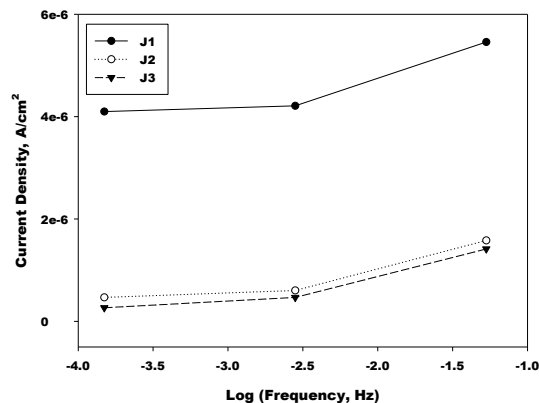
$$R_p = \beta_a \beta_c / (\beta_a + \beta_c) / 2.303 j_{cor} \quad (9)$$



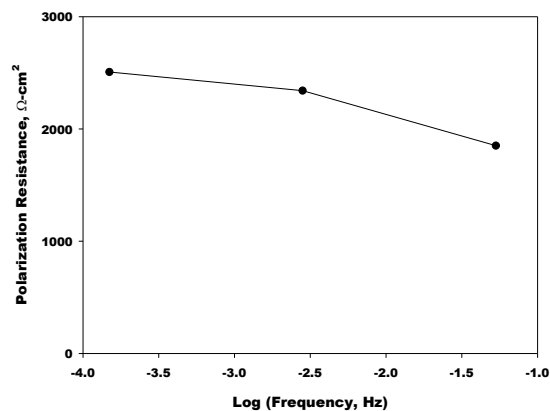


(b)

Figure 3. Plots of harmonic current (a) and polarization resistance (b) vs. frequency at the corrosion potential for a type 316 stainless steel in 2 % NaCl (pH=1.6) solution.



(a)



(b)

Figure 4. Plots of harmonic current (a) and polarization resistance (b) vs. frequency at the corrosion potential for a type 316 stainless steel in 2 % NaCl (pH=1.9).

As can be seen in these Figs., harmonic currents j_1 , j_2 and j_3 increase, and polarization resistance

decreases with increasing frequency in two solutions. The increase of harmonic current with frequency is consistent with a previous work [11]. Higher polarization resistance is again observed in the solution with pH=1.9 compared to that in solution of pH=1.6 as in table 1, which is consistent with the trend shown in the results of the d. c. polarization and electrochemical impedance measurements.

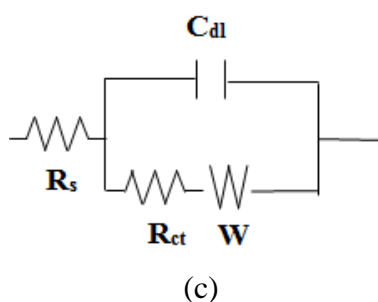
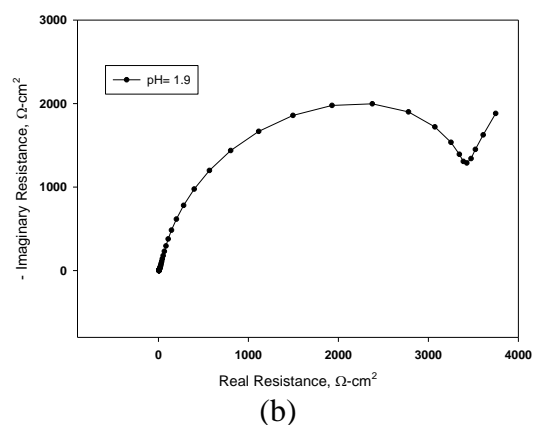
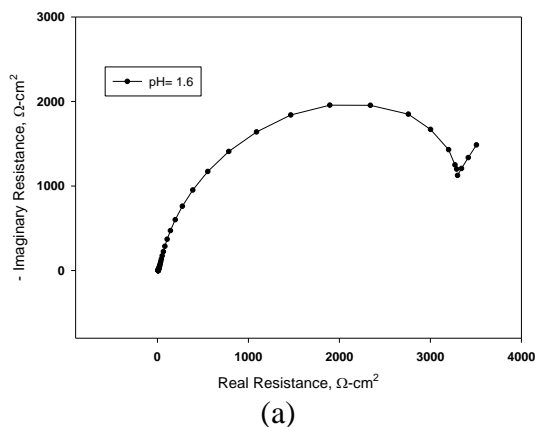


Figure 5. Nyquist plots for a type 316 stainless steel under mixed control condition in 2 % NaCl solutions with pH 1.6 (a) and 1.9 (b), and an equivalent circuit (c).

In addition, values of the polarization resistance determined from harmonic currents at 0.1 Hz are closer to those from d. c. polarization and electrochemical impedance measurements. The frequency that gives a value of polarization resistance close to that from other tests is similar to that in early works [4,7,13]. The values of polarization resistance at 0.1 Hz are 1706.3 and 1851.0 $\Omega\text{-cm}^2$ in solutions with pH 1.6 and 1.9, respectively, which are higher compared to those from d. c. polarization and electrochemical impedance measurements.

Table 1. Polarization resistance determined from harmonic current measurement.

	Polarization resistance ($\Omega\text{-cm}^2$)		
	0.001 Hz	0.01 Hz	0.1 Hz
2 % NaCl, pH 1.6	2113.5	2092.5	1706.3
2 % NaCl, pH 1.9	2507.7	2341.6	1851.0

3.2 Harmonic current in mixed control condition

Figs. 5 (a) and (b) show the EIS Nyquist plots obtained immediately after potentiostatic polarization for 600 s at a potential more positive than corrosion potential by 150 mV in 2.0 % NaCl solutions with pH 1.6 and 1.9, respectively. The Nyquist plots are composed of capacitive arcs and straight lines. As was described previously, the arc in high frequency region represents the effects of charge transfer at the specimen-solution interface. The straight line in low frequency region shows the presence of diffusion component in corrosion. The spectra could be best fitted with an equivalent circuit in Fig. 5(c).

Diffusion element W that appears in Fig. 5(c) is the Warburg diffusion element. This is a common diffusion circuit element used to model semi-infinite linear diffusion, that is, unrestricted diffusion to a large planar electrode. The fitting parameters obtained from the circuit are listed in table 2. A parameter Y_o in the table is the admittance at the angular frequency $\omega = 1$ rad/s (0.16 Hz) and related to Warburg coefficient σ , and impedance Z_w by the relations,

$$Y_o = 1/(\sqrt{2} \sigma) \tag{10}$$

$$Z_w = \sigma/\omega^{1/2} - j\sigma/\omega^{1/2} \tag{11}$$

Table 2. Electrochemical parameters obtained from fitting the circuit in Fig. 5(c).

	R_s ($\Omega \text{ cm}^2$)	C_{dl} (F)	R_{ct} ($\Omega \text{ cm}^2$)	Y_o ($\Omega^{-1} \text{ s}^{1/2}$)
2 % NaCl, pH 1.6	7.8	8.7×10^{-5}	2501	11.5×10^{-4}
2 % NaCl, pH 1.9	8.6	9.6×10^{-5}	2687	14.3×10^{-4}

As can be seen in this table, the values of C_{dl} and Y_o tend to increase with pH, and higher R_{ct} is observed in the solution of pH=1.9. The trend in change of R_{ct} with pH is consistent with that in charge transfer condition.

Fig. 6 represents the results of harmonic current measurements as a function of frequency obtained immediately after potentiostatic polarizations for 600 s at a potential 150 mV more positive than the corrosion potential. The corrosion current density and polarization resistance could not be determined from the results of harmonic current measurements since no explicit relations are known yet for the corrosion under mixed control of charge transfer and diffusion. As can be seen in these Figs., harmonic currents j_1 , j_2 and j_3 tend to increase with increasing frequency in two solutions. The trend of change in harmonic currents with frequency is similar to that in charge transfer control

condition [13]. Since no specific attention was given to the test conditions in the previous works, comparison of these results with those works is not available.

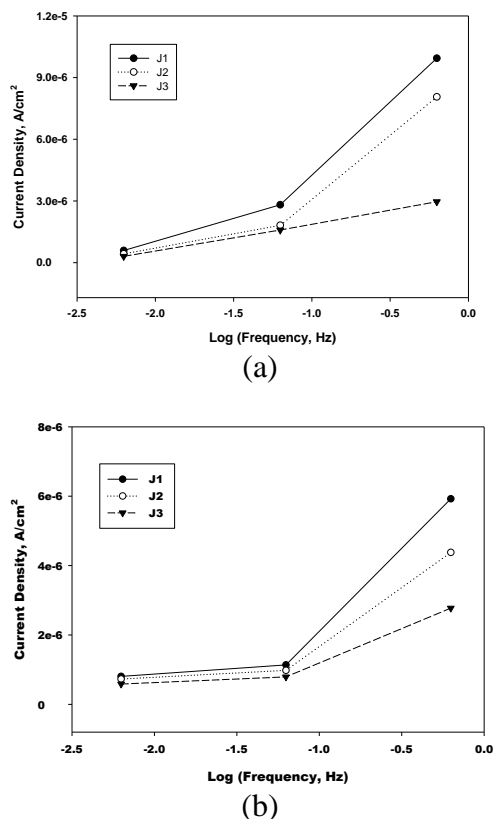


Figure 6. Plots of harmonic current vs. applied frequency under mixed control condition for a type 316 stainless steel in 2 % NaCl with pH 1.6 (a) and 1.9 (b) solutions.

3.3 Analysis of the slope

Fig. 7 shows the plots of the square of harmonic current j_i^2 vs. the square of frequency ω^2 at the corrosion potential in 2 % NaCl solutions. The slopes of j_1^2 , j_2^2 and j_3^2 in these plots represent the values of $C_{dl}^2 E_o^2$ as in equation (12), which can also be determined from EIS data. The frequency dependence of harmonic current results from the existence of capacitance in charge transfer condition and is given by [13],

$$j_i(\omega)^2 = j_i(0)^2 + \omega^2 C_{dl}^2 E_o^2 \quad (12)$$

where $j_i(0)$ and $j_i(\omega)$ are harmonic currents at the frequency 0 and ω , respectively.

Comparison of the values of $C_{dl}^2 E_o^2$ in NaCl solution with pH 1.6 (table 3) reveals that the values determined from the slope of the plot is roughly 6 times those from EIS data in j_1 , and they are very close in j_2 and j_3 , the difference being less than 70 %. A similar trend is observed in 2 % NaCl solution with pH 1.9. In this solution, the values determined from the slope of the plot is about 7 times those from EIS data in j_1 , and they are again very close in j_2 and j_3 , the difference being less than 30 %.

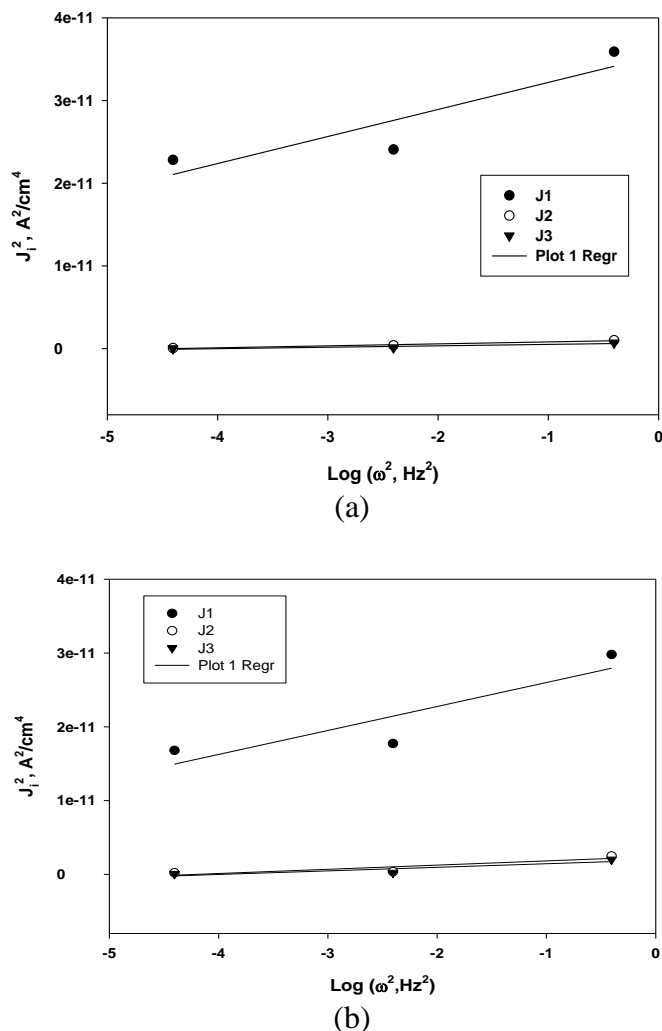


Figure 7. Frequency dependence of harmonic currents at the corrosion potential for a type 316 stainless steel in 2 % NaCl with pH= 1.6 (a) and 1.9 (b) solutions.

Table 3. Comparison of values of $C_{dl}^2 E_0^2 (F^2 V^2)$ determined at the corrosion potential from harmonic current measurements and EIS in 2 % NaCl solutions.

		$C_{dl}^2 E_0^2 (A^2 s^2)$	
		Harmonic/Slope	EIS
2 % NaCl pH =1.6	j_1^2	3.2×10^{-11}	5.3×10^{-12}
	j_2^2	2.0×10^{-12}	5.3×10^{-12}
	j_3^2	1.6×10^{-12}	5.3×10^{-12}
2 % NaCl pH =1.9	j_1^2	3.2×10^{-11}	4.4×10^{-12}
	j_2^2	5.6×10^{-12}	4.4×10^{-12}
	j_3^2	4.7×10^{-12}	4.4×10^{-12}

Fig. 8 represents the dependence of the square of the first harmonic current, j_1^2 on the square of frequency, ω^2 under mixed control condition. Only the results of j_1^2 are analyzed since the difference in values determined from harmonic current and EIS is the largest in the first harmonic current. The

values of $C_{dl}^2 E_o^2$ determined from the slope of the plot and EIS are 2.4×10^{-10} and $7.6 \times 10^{-13} \text{ A}^2 \text{ s}^2$ or Ampere-sec, respectively, in 2 % NaCl solution with pH 1.6 as in table 4. The former is about 300 times that of the latter. In 2 % NaCl solution with pH 1.9, the values of $C_{dl}^2 E_o^2$ determined from the slope of the plot and EIS are 8.7×10^{-11} and $9.1 \times 10^{-13} \text{ A}^2 \text{ s}^2$, respectively. The former is about 100 times that of the latter. Thus, the frequency dependence on harmonic current may not be adequately predicted by equation 12.

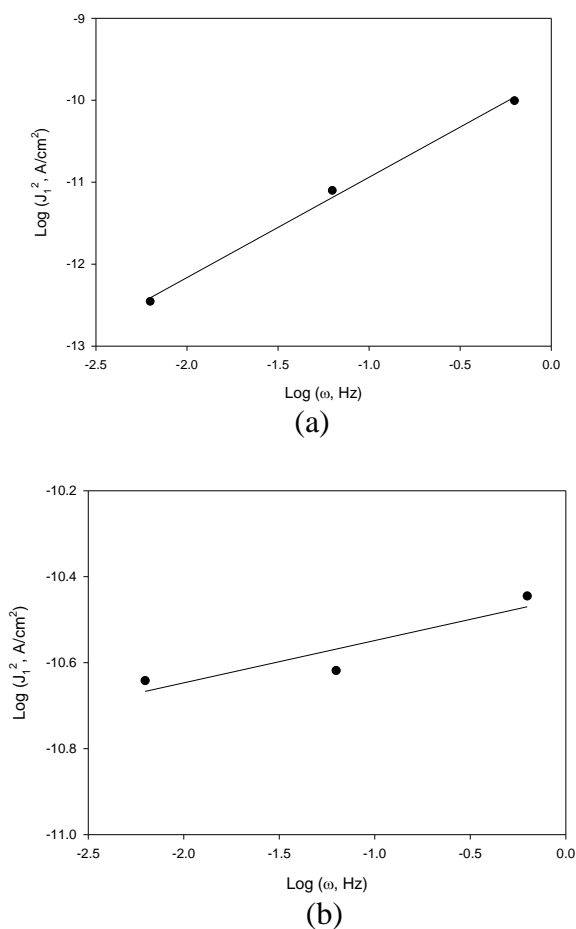


Figure 8. Frequency dependence of the first harmonic current under mixed control condition for a type 316 stainless steel in 2 % NaCl with pH 1.6 (a) and 1.9 (b) solutions.

Table 4. Comparison in values of $C_{dl}^2 E_o^2$ and E_o^2/σ^2 determined from harmonic current measurements and EIS under mixed control condition in 2 % NaCl solutions.

	$C_{dl}^2 E_o^2 \text{ (A}^2 \text{ s}^2\text{)}$		$E_o^2/\sigma^2 \text{ (A}^2 \text{ s}^2\text{)}$	
	Harmonic/Slope	EIS	Harmonic/Slope	EIS
2 % NaCl (pH 1.6)	2.4×10^{-10}	7.6×10^{-13}	1.6×10^{-10}	2.6×10^{-10}
2 % NaCl (pH 1.9)	8.7×10^{-11}	9.1×10^{-13}	2.1×10^{-11}	4.0×10^{-10}

Summarizing the effects of frequency on harmonic currents, the values $C_{dl}^2 E_o^2$ determined from the slope of the plot is roughly 6 to 7 times that determined from EIS at the corrosion potential or under charge transfer condition. However, the former is about 100 to 300 times that of the latter under mixed control condition. This confirms that the square of harmonic currents j_i^2 are linearly dependent on the square of frequency, ω^2 in charge transfer condition as in equation 12, but not on the square of frequency in mixed control condition. The square of harmonic currents increases at different rates from those predicted from equation 12 as shown in table 4. Thus, a new equation is needed to be developed to evaluate the frequency dependence of harmonic currents in mixed control condition.

For the development of an equation in mixed control condition, Warburg coefficient σ was used instead of C_{dl} . Since harmonic current increases with frequency, the relation expressing the frequency dependence should contain the term that is proportional to frequency or to a positive power of frequency. By a dimensional analysis, a term for frequency dependence having the dimension of current density, A/cm^2 is $\omega E_o^2 / \sigma^2$. By analogy with equation 12, frequency dependence of harmonic current can be expressed by,

$$j_i(\omega)^2 = j_i(0)^2 + \omega E_o^2 / \sigma^2 \quad (13)$$

This equation predicts a linear dependence of the square of harmonic current j_i^2 on the frequency ω in mixed control condition.

The value of E_o^2 / σ^2 determined from EIS data using equation 13 is $2.6 \times 10^{-10} A^2 s$, and that measured from the slope of the plot is $1.6 \times 10^{-10} A^2 s$ in 2 % NaCl (pH=1.6) solution. The former is very close to the latter, that is, about 1.6 times that of the latter. In 2 % NaCl (pH=1.9) solution, the value of E_o^2 / σ^2 determined from EIS data using equation 13 is $4.0 \times 10^{-10} A^2 s$, and that taken from the slope is $2.1 \times 10^{-11} A^2 s$. The former is less than 20 times that of the latter. Thus, the use of equation 13 enables the prediction of the frequency dependence of harmonic currents in mixed control condition with accuracy comparable to that determined using equation 12 in charge transfer control condition.

A linear dependence of the square of the harmonic current j_i^2 on the frequency ω in equation 13 under mixed control condition is, however, in contrast to that in a previous work [3], in which the square of harmonic current is roughly predicted to be inversely proportional to the square root of frequency. This may suggest the frequency dependence of harmonic current varies with corrosion systems. In the work [3], the validity was confirmed only in a mild steel in Na_2SO_4 solution, and the equation for the frequency dependence of harmonic current includes Bessel functions, surface concentration and diffusion coefficient of oxidant as well. Evaluation of the frequency dependence of harmonic current is thus more complicated compared to equation 13 developed in this work which includes only Warburg coefficient σ . This coefficient can be easily measured by EIS.

4. CONCLUSIONS

The frequency dependence of harmonic current was investigated in a type 316 stainless steel in NaCl solutions. Harmonic currents j_1 , j_2 and j_3 increase, and polarization resistance decreases in pH 1.6 and pH 1.9 solutions with increasing frequency in charge transfer condition. Harmonic currents increase with frequency, but at different rates in mixed control condition of charge transfer and

diffusion.

The square of harmonic currents j_i^2 is linearly dependent on the square of frequency, ω^2 in charge transfer condition, but not on the square of frequency in mixed control condition. An equation was developed by a dimensional analysis that best fits the experimental data. According to this equation, a linear dependence of square of harmonic currents j_i^2 on the frequency ω is predicted in mixed control condition.

References

1. J. Devay, L. Meszaros, *Acta Chim. Acad. Sci. Hung.* 100(1–4) (1979) 183.
2. J. S. Gill, L. M. Callow, J. D. Scantlebury, *Corrosion* 39 (2) (1983) 61.
3. R. W. Bosch, W. E. Bogaerts, *J. Electrochem. Soc.* 143 (12) (1996) 4033.
4. W. Durnie, R. D. Marco, A. Jefferson and B. Kinsella, *Corros. Sci.*, 44 (2002) 1213.
5. S. Richter, R. I. Thorarinsdottir, F. Jonsdottir, *Corros. Sci.*, 49(4) (2007) 1907.
6. E. Tada, K. Noda, S. Kumai, *Corros. Sci.*, 46(6) (2004) 1549.
7. L. Meszaros, G. Meszaros, B. Lengyel, *J. Electrochem. Soc.* 141 (8) (1994) 2068.
8. S. Sathiyarayanan, G. Venkatachari, N.S. Rengaswamy, K. Balakrishnan, *Proceedings, 13th International Corrosion Congress*, Melbourne, (1996) p. 5.
9. B. Rosborg, J. Pan, C. Leygraf, *Corros. Sci.*, 47(12) (2005) 3267.
10. M. C. H. McKubre and B. C. Syrett, *ASTM STP 908*, ASTM, Philadelphia, (1986) p. 5.
11. K. L. Dawson and J. D. Scantlebury, *Mats. Sci. Forum*, 44 & 45 (1989) 387
12. R. Vedalakshmi, SP. Manoharan and H. Song and N. Palaniswamy, *Corr. Sci.*, 51 (2009) 2777
13. S. Sathiyarayanan and K. Balakrishnan, *Brit. Corr. J.*, 29(2), (1994) 152.

© 2014 The Authors. Published by ESG (www.electrochemsci.org). This article is an open access article distributed under the terms and conditions of the Creative Commons Attribution license (<http://creativecommons.org/licenses/by/4.0/>).